QCD Phase Transition in the Chiral Limit

O. Kaczmarek, F. Karsch, A. Lahiri, L. Mazur, C. Schmidt

published in

NIC Symposium 2020
M. Müller, K. Binder, A. Trautmann (Editors)

Forschungszentrum Jülich GmbH,
John von Neumann Institute for Computing (NIC),
Schriften des Forschungszentrums Jülich, NIC Series, Vol. 50,
ISBN 978-3-95806-443-0, pp. 193.
http://hdl.handle.net/2128/24435

QCD Phase Transition in the Chiral Limit

Olaf Kaczmarek, Frithjof Karsch, Anirban Lahiri, Lukas Mazur, and Christian Schmidt

Fakultät für Physik, Universität Bielefeld, 33501 Bielefeld, Germany
E-mail: karsch@physik.uni-bielefeld.de

We present a lattice QCD based determination of the chiral phase transition temperature in QCD with two massless (up and down) and one strange quark having its physical mass. We propose and calculate two novel estimators for the chiral transition temperature for several values of the light quark masses, corresponding to Goldstone pion masses in the range of $58\ \mathrm{MeV} \lesssim m_\pi \lesssim 163\ \mathrm{MeV}$. The chiral phase transition temperature is determined by extrapolating to vanishing pion mass using universal scaling analysis. After thermodynamic, continuum and chiral extrapolations we find the chiral phase transition temperature $T_c^0 = 132^{+3}_{-6}$ MeV. We also present some preliminary calculations on interplay of effective $U_A(1)$ restoration and chiral phase transition towards chiral limit.

1 Introduction

For physical values of the two light (up and down) and one heavier (strange) quark masses strongly interacting matter undergoes a crossover from a low temperature hadronic regime to a high temperature region that is best described by quark and gluon degrees of freedom. This smooth crossover between the two asymptotic regimes is not a phase transition.[1] It is characterised by a pseudo-critical temperature, T_{pc}, that has been determined in several numerical studies of Quantum Chromodynamics (QCD).[2–4] A recent determination of T_{pc} using the maximal fluctuations of several chiral observables gave $T_{pc} = (156.5 \pm 1.5)$ MeV.[5] On the contrary to the calculation for physical masses, till date one of the outstanding challenges in QCD thermodynamics is to clarify the nature of the QCD phase transition that exists in the chiral limit, *i. e.* in the limit of vanishing light quark masses, $(m_u, m_d) \to (0, 0)$. While it is widely expected that the chiral phase transition at vanishing values of the two light quark masses is a second-order transition, belonging to the $O(4)$ universality class, a subtle role is played by the $U(1)_A$ axial anomaly.[6] If the $U(1)_A$ symmetry, which is broken in the QCD vacuum, does not get "effectively restored" at high temperature, the transition indeed will be in the universality of 3-d, $O(4)$ spin models. However, if the $U(1)_A$ symmetry breaking effects are small already at the chiral phase transition, at which the chiral condensate vanishes, the phase transition may turn out to be first order,[6] although a second-order transition belonging to larger 3-d universality class[7–10] may become of relevance. If the chiral phase transition is first order then a second order phase transition, belonging to the 3-d $Z(2)$ universality class, would occur for $m_l^c > 0$. When decreasing the light to strange quark mass ratio, $H = m_l/m_s$, towards zero, this would give rise to diverging susceptibilities already for some critical mass ratio $H_c = m_l^c/m_s > 0$.

2 Determination of Chiral Phase Transition Temperature

2.1 Observables

In QCD chiral symmetry is spontaneously broken at low temperatures The corresponding order parameter named chiral condensate is obtained as the derivative of the partition function, $Z(T, V, m_u, m_d, m_s)$, with respect to the quark mass m_f of flavour f,

$$\langle\bar{\psi}\psi\rangle_f = \frac{T}{V}\frac{\partial \ln Z(T, V, m_u, m_d, m_s)}{\partial m_f} \tag{1}$$

In the chiral limit, $m_l \to 0$, the light quark chiral condensate, $\langle\bar{\psi}\psi\rangle_l = (\langle\bar{\psi}\psi\rangle_u + \langle\bar{\psi}\psi\rangle_d)/2$, is an exact order parameter for the chiral phase transition. We take care of additive and multiplicative renormalisation by introducing[3] a combination made out of the light and strange quark chiral condensates,

$$M = 2\left(m_s\langle\bar{\psi}\psi\rangle_l - m_l\langle\bar{\psi}\psi\rangle_s\right)/f_K^4 \tag{2}$$

where $f_K = 156.1(9)/\sqrt{2}$ MeV, is the kaon decay constant, which we use as normalisation constant to define a dimensionless order parameter M. The derivative of M with respect to the light quark masses defines the renormalised chiral susceptibility,

$$\begin{aligned}\chi_M &= m_s(\partial_{m_u} + \partial_{m_d})M|_{m_u=m_d} \\ &= m_s(m_s\chi_l - 2\langle\bar{\psi}\psi\rangle_s - 4m_l\chi_{su})/f_K^4\end{aligned} \tag{3}$$

with $\chi_{fg} = \partial_{m_f}\langle\bar{\psi}\psi\rangle_g$ and $\chi_l = 2(\chi_{uu} + \chi_{ud})$. M and χ_M are renormalisation group invariant quantities when terms proportional to the logarithm of light quark masses can be neglected.

Near a 2^{nd} order phase transition M and χ_M can be described by universal finite-size scaling functions $f_G(z, z_L)$ and $f_\chi(z, z_L)$ where the scaling variables in arguments are defined as $z = t/h^{1/\beta\delta}$ and $z_L = l_0/(Lh^{\nu/\beta\delta})$, with $t = (T - T_c^0)/(t_0T_c^0)$ being the reduced temperature; $h = H/h_0$ with $H = m_l/m_s$ denotes the symmetry breaking field and L being the linear extent of the system, $L \equiv V^{1/3}$. The normalisation constants $t_0,\ h_0$ and l_0 that appear in the definition of the scaling variables are non-universal parameters. Before approaching the chiral limit, one also needs to take a proper thermodynamic limit, $V \to \infty$ of any calculation.

Although close to a critical point at $(z, z_L) = (0, 0)$, M and χ_M can be described by the universal scaling functions, but away from the critical point they also receive contributions from corrections-to-scaling[11, 12] and regular terms. With this we may write

$$\begin{aligned}M &= h^{1/\delta}f_G(z, z_L) + f_{sub}(T, H, L) \\ \chi_M &= h_0^{-1}h^{1/\delta-1}f_\chi(z, z_L) + \tilde{f}_{sub}(T, H, L)\end{aligned} \tag{4}$$

where $f_{sub}(T, H, L)$ and $\tilde{f}_{sub}(T, H, L)$ denotes the above-mentioned sub-leading contributions for M and χ_M respectively.

A commonly defined estimator for pseudo-critical temperature corresponds to the peak in the scaling function $f_\chi(z, z_L)$ for large enough system sizes. Within the scaling regime the peak is located at $z = z_p(z_L)$, which defines T_p,[3]

$$T_p(H, L) = T_c^0\left(1 + \frac{z_p(z_L)}{z_0}H^{1/\beta\delta}\right) + \text{sub-leading} \tag{5}$$

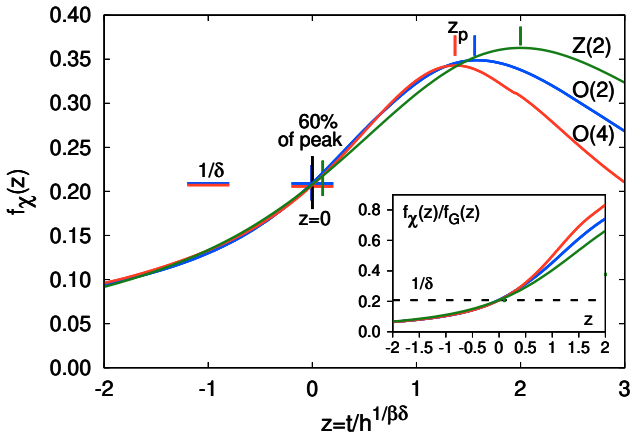

Figure 1. Scaling functions for the 3-d $Z(2)$, $O(2)$ and $O(4)$ universality classes. The position z_p of the peak of the scaling functions (vertical lines) and the position z_{60} where the scaling function attains 60 % of its maximal value (crosses) are shown. Lines close to $z = -1$ show $1/\delta$ for these three universality classes, which agree to better than 1 %. The inset shows the ratio of scaling functions, $f_\chi(z)/f_G(z)$, used in determinations of the chiral phase transition temperature.

with $z_0 = h_0^{1/\beta\delta}/t_0$. The first term accounts for the universal quark mass dependence of T_p. Apart from that contributions from corrections-to-scaling and regular terms will be there, shifting the peak-location of the chiral susceptibilities. These contributions together have been denoted as "sub-leading" in Eq. 5.

Depending on the magnitude of $z_p/z_0 \equiv z_p(0)/z_0$, $T_p(H,L)$ may change significantly with H, when approaching towards the chiral limit.[3] So the contribution from the sub-leading terms will be non-negligible which in turn makes the chiral extrapolation non-trivial. Moreover one has to deal with more non-universal parameters. Thus it will be really advantageous to determine T_c^0 from scaling of such estimators which are defined with $z \simeq 0$. Then by construction $T_p(H,L)$ will have a way milder H dependence which results in rather easier to control $H \to 0$ extrapolation to calculate T_c^0.

Here we consider two such estimators[13, 14] for T_c^0, defined close to or at $z = 0$, in the thermodynamic limit. We define temperatures T_δ and T_{60} through the following conditions:

$$\frac{H\chi_M(T_\delta,H,L)}{M(T_\delta,H,L)} = \frac{1}{\delta} \tag{6}$$

$$\chi_M(T_{60},H) = 0.6\chi_M^{max} \tag{7}$$

The ratio on the LHS of Eq. 6 has already been introduced in Ref. 15 as a tool to analyse the chiral transition in QCD. T_{60} will correspond to the temperature left to the peak of χ_M; *i. e.* $T_{60} < T_p$. These pseudo-critical temperatures T_X, defined through Eq. 6 and Eq. 7, are already close to T_c^0 for finite H and L^{-1} because they involve $z_X(z_L)$ which either vanishes or stays close to zero in the $L^{-1} \to 0$ limit. To be precise, $z_\delta \equiv z_\delta(0) = 0$ and $z_{60} \equiv z_{60}(0) \simeq 0$. Some values for z_{60}, along with the corresponding scaling functions in the thermodynamic limit have been shown in Fig. 1 for relevant universality classes.

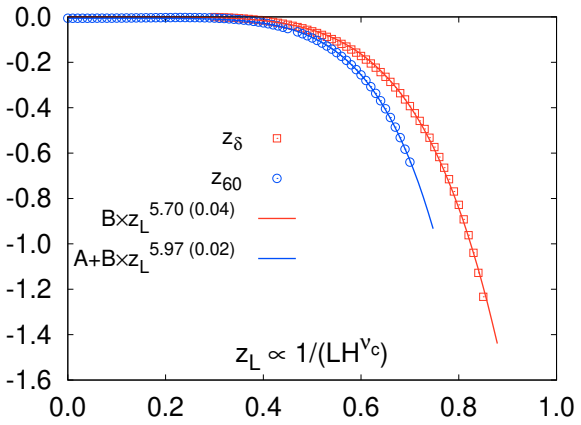

Figure 2. Universal functions $z_\delta(z_L)$ and $z_{60}(z_L)$ calculated from the finite-size scaling functions $f_G(z, z_L)$, $f_\chi(z, z_L)$ determined in Ref. 16.

Ignoring possible contributions from corrections-to-scaling, and keeping in f_{sub} only the leading T independent, infinite volume regular contribution proportional to H, we then find for the pseudo-critical temperatures,[13]

$$T_X(H,L) = T_c^0 \left(1 + \left(\frac{z_X(z_L)}{z_0}\right) H^{1/\beta\delta}\right) + c_X H^{1-1/\delta+1/\beta\delta} \quad , \quad X = \delta,\ 60 \qquad (8)$$

The universal functions, $z_X(z_L)$ may directly be determined from the ratio of the scaling functions $f_\chi(z_\delta, z_L)/f_G(z_\delta, z_L) = 1/\delta$ and $f_\chi(z_{60}, z_L)/f_\chi(z_p, z_L) = 0.6$, respectively. In Fig. 2 we show the calculation of the universal functions $z_X(z_L)$ along with the optimal parameterised form, for the 3-d, $O(4)$ universality class using the finite-size scaling functions $f_G(z, z_L)$, $f_\chi(z, z_L)$ determined in Ref. 16.

We will present here results on T_δ and T_{60} obtained in lattice QCD calculations.[13] We calculated the chiral order parameter M and the chiral susceptibility χ_M (Eqs. 2 and 3) in $(2+1)$-flavour QCD with degenerate up and down quark masses ($m_u = m_d$). Our calculations are performed with the Highly Improved Staggered Quark (HISQ) action[17] in the fermion sector along with the Symanzik improved gluon action. The strange quark mass has been tuned to its physical value[18] and the light quark mass has been varied in a range $m_l \in [m_s/160 : m_s/20]$ corresponding to Goldstone pion masses in the range 58 MeV$\lesssim m_\pi \lesssim$163 MeV. At each temperature we performed calculations on lattices of size $N_\sigma^3 N_\tau$ for three different values of the lattice cut-off, $aT = 1/N_\tau$, with $N_\tau = 6,\ 8$ and 12. The spatial lattice extent, $N_\sigma = L/a$, has been varied in the range $4 \leq N_\sigma/N_\tau \leq 8$. For each N_τ we analysed the volume dependence of M and χ_M in order to perform controlled infinite volume extrapolations.

2.2 Results

We show results for χ_M in Fig. 3, on lattices with temporal extent $N_\tau = 8$ for 5 different values of the quark mass ratio, $H = m_l/m_s$, and the largest lattice available for each H.

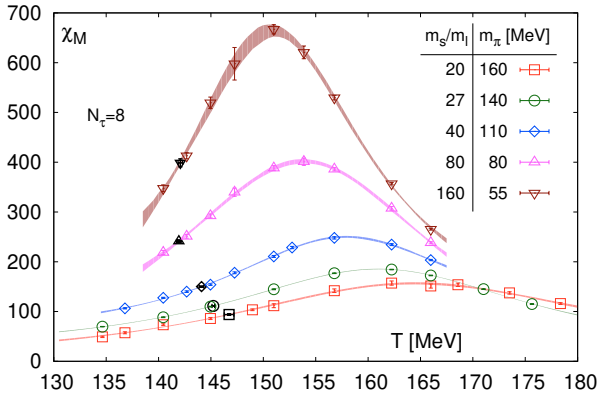

Figure 3. Quark mass dependence of the chiral susceptibility on lattices with temporal extent $N_\tau = 8$ for several values of the light quark masses. The spatial lattices extent N_σ is increased as the light quark mass decreases: $N_\sigma = 32$ $(H^{-1} = 20,\ 27)$, 40 $(H^{-1} = 40)$, 56 $(H^{-1} = 80,\ 160)$. Black symbols mark the points corresponding to 60 % of the peak height. Figure taken from Ref. 13.

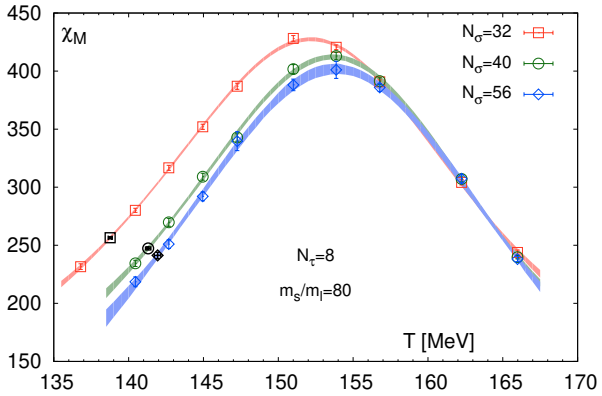

Figure 4. Volume dependence of the chiral susceptibility on lattices with temporal extent $N_\tau = 8$ for three different spatial lattice sizes at $H = 1/80$. Black symbols mark the points corresponding to 60 % of the peak height. Figure taken from Ref. 13.

The increase of the peak height, χ_M^{max}, with decreasing H is consistent with the expected behaviour, $\chi_M^{max} \sim H^{1/\delta-1} + const.$, with $\delta \simeq 4.8$ within rather large uncertainty which restricts a precise determination of δ.

In Fig. 4 we show the volume dependence of χ_M for $H = 1/80$ on lattices with temporal extent $N_\tau = 8$ and for $N_\sigma/N_\tau = 4,\ 5$ and 7. Similar results have also been obtained for $N_\tau = 6$ and 12. It is important to note that χ_M^{max} decreases slightly with increasing volume, contrary to what one would expect to find at or close to a 1^{st} order phase transition. In fact, this trend seems to be consistent with the behaviour seen for

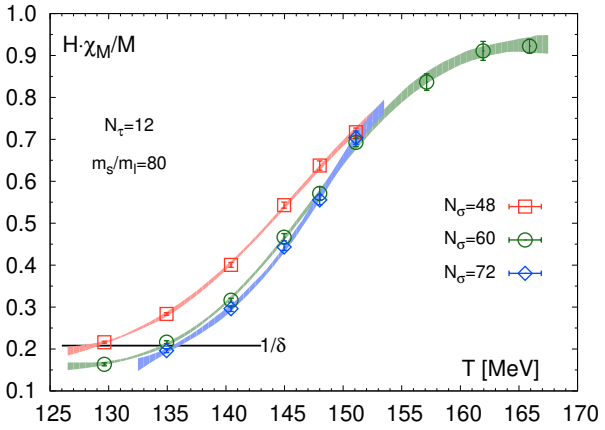

Figure 5. The ratio $H\chi_M/M$ versus temperature for $N_\tau = 12$, $m_l/m_s = 1/80$ and different spatial volumes. Figure taken from Ref. 13.

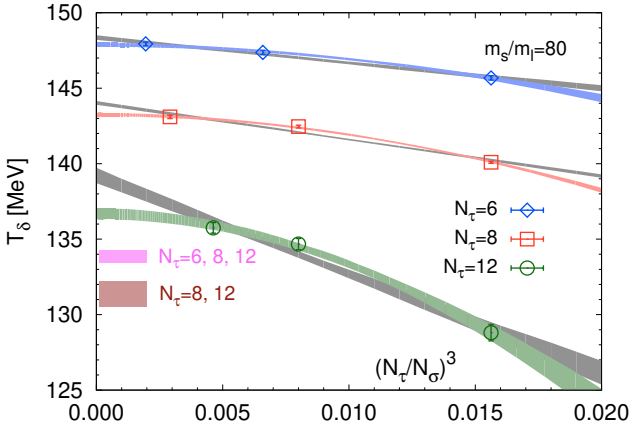

Figure 6. Infinite volume extrapolations based on an $O(4)$ finite-size scaling ansatz (coloured bands) and fits linear in $1/V$ (grey bands). Horizontal bars show the continuum extrapolated results for $H = 1/80$. Figure taken from Ref. 13.

$O(4)$ universality class finite-size scaling functions.[16] Our current results, thus, suggest a continuous phase transition at $H_c = 0$.

Using results for χ_M and M we constructed the ratios $H\chi_M/M$ for different lattice sizes and several values of the quark masses. In Fig. 5 this ratio has been shown on the $N_\tau = 12$ lattices with $H = 1/80$ which is the lowest mass for this N_τ. The intercepts with the horizontal line at $1/\delta$ define $T_\delta(H, L)$. For $H = 1/80$ and each of the N_τ, we have results for three different volumes on which we can extrapolate $T_\delta(H, L)$ to the thermodynamic limit. We performed such extrapolations using (i) the $O(4)$ ansatz given

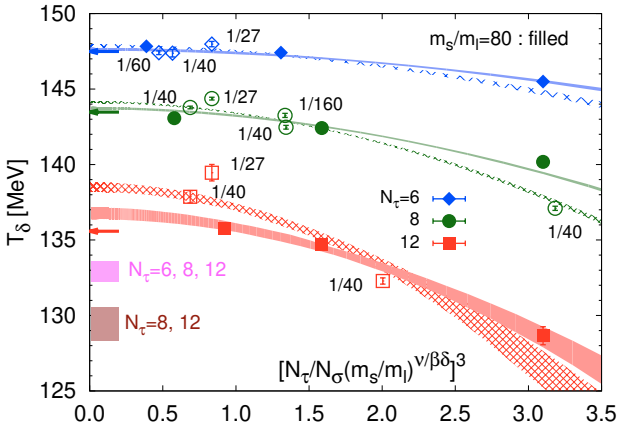

Figure 7. Finite size scaling fits for T_δ based on all data for $H \leq 1/27$ and all available volumes. Arrows show chiral limit results at fixed N_τ and horizontal bars show the continuum extrapolated results for $H = 0$. Figure taken from Ref. 13.

in Eq. 8 which is appropriate when the singular part dominates the partition function and (ii) an extrapolation in $1/V$ which is appropriate if, for large L, the volume dependence predominantly arises from regular terms. In the former case we use the approximation $z_\delta(z_L) \sim z_L^{5.7}$, as shown in Fig. 2. This parameterises well the finite-size dependence of T_δ in the scaling regime. The resulting volume extrapolations are shown in Fig. 6. For fixed H the results tend to approach the infinite volume limit more rapidly than $1/V$, which is in agreement with the behaviour expected from the ratio of finite-size scaling functions. The resulting continuum limit extrapolations in $1/N_\tau^2$ based on data with and without $N_\tau = 6$ are shown as horizontal bars in this figure. A similar analysis is performed for $H = 1/40$. Finally, we extrapolate the continuum results for $T_\delta(H, \infty)$ with $H = 1/40$ and $1/80$ to the chiral limit using Eq. 8 with $z_\delta(0) = 0$. Results obtained from these extrapolation chains, which involve either an $O(4)$ or $1/V$ ansatz for the infinite volume extrapolation, and continuum limit extrapolations performed using all three N_τ or the two largest N_τ, lead to chiral transition temperatures T_c^0 in the range (128-135) MeV. A complete summary of the resulting values for T_c^0 are depicted in Fig. 8.

Since the fits in Fig. 6 suggest that the $O(4)$ scaling ansatz is appropriate to account for the finite volume effects already at finite N_τ, we can attempt a joint infinite volume and chiral extrapolation of all data available for different light quark masses and volumes at fixed N_τ. This utilises the quark mass dependence of finite-size corrections, expressed in terms of z_L. The main difference of this method from the earlier one is that chiral extrapolation is done before taking the continuum limit. Using the scaling ansatz given in Eq. 8, it also allows to account for the contribution of a regular term in a single fit. Fits for fixed N_τ based on this ansatz, using data for all available lattice sizes and $H \leq 1/27$, are shown in Fig. 7. Bands for $H = 1/40$ and $1/80$ are shown in the figure. As can be seen, for $H = 1/80$, these bands compare well with the fits shown in Fig. 6. For each N_τ an arrow shows the corresponding chiral-limit result, $T_\delta(0, \infty)$. We extrapolated these chiral-limit results to the continuum limit and estimated systematic errors again by including or leaving

out data for $N_\tau = 6$. The resulting T_c^0, shown in Fig. 8, are in complete agreement with the corresponding numbers obtained by first taking the continuum limit and then taking the chiral limit. Within the current accuracy these two limits are interchangeable.

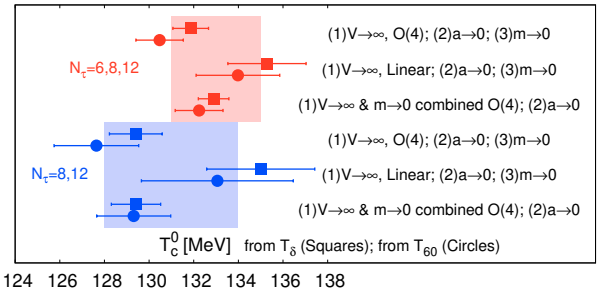

Figure 8. Summary of fit results. The order of different limits taken, described in the main text, is written beside each pair of closest points. For such a pair squares stands for calculations using T_δ and circles stands for calculations using T_{60}. The upper half of the points corresponds to the calculations when continuum extrapolation uses all three N_τ and is presented in red. Similarly the lower half, presented in blue, corresponds to the calculations where only two largest N_τ have been used in the continuum extrapolation. Figure taken from Ref. 13.

Similarly, we analysed results for T_{60} on all data sets following the same strategy as for T_δ. As can be seen in Fig. 8, we find for each extrapolation ansatz that the resulting values for T_c^0 agree to better than 1 % accuracy with the corresponding values from T_δ. This suggests that the chiral susceptibilities used for this analysis reflect basic features of the $O(4)$ scaling functions.

Performing continuum extrapolations by either including or discarding results obtained on the coarsest ($N_\tau = 6$) lattices leads to a systematic shift of about (2-3) MeV in the estimates for T_c^0. This is reflected in the displacement of the two coloured bands in Fig. 8, which show averages for T_c^0 obtained with our different extrapolation ansätze. Averaging separately over results for T_δ and T_{60} obtained with both, continuum extrapolation procedures and including this systematic effect, we find for the chiral phase transition temperature,

$$T_c^0 = 132^{+3}_{-6}\ \mathrm{MeV} \tag{9}$$

3 Towards an Understanding of Anomalous $U_A(1)$ Symmetry Restoration

3.1 Observable

The chiral susceptibility, defined after Eq. 3 receives contributions from a disconnected and connected part which are related to quark-line disconnected and connected Feynman diagrams,[3] *i. e.*

$$\chi_l = \chi_{l,disc} + \chi_{l,conn} \tag{10}$$

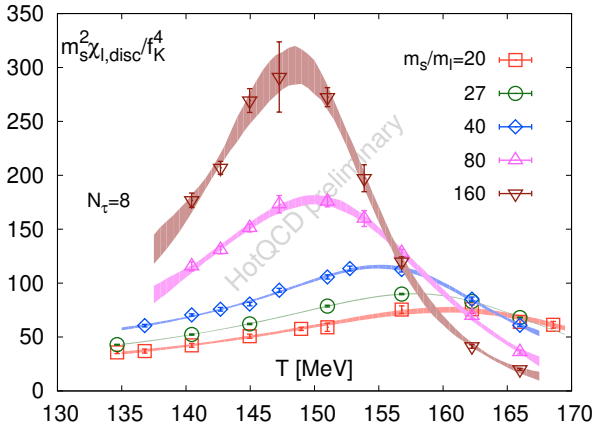

Figure 9. The disconnected chiral susceptibility obtained from calculations in (2+1)-flavour QCD with the HISQ action on lattices of $N_\tau = 8$, at several values of the light quark mass. The susceptibility has been multiplicatively renormalised by multiplying with the square of the strange quark mass and the kaon decay constant f_K has been used to set the scale for the susceptibility as well as the temperature.

with

$$\chi_{l,disc} = \frac{N_f^2}{16 N_\sigma^3 N_\tau} \left\{ \langle \left(\mathrm{Tr} D_l^{-1} \right)^2 \rangle - \langle \mathrm{Tr} D_l^{-1} \rangle^2 \right\} \quad \text{and} \tag{11}$$

$$\chi_{l,conn} = -\frac{N_f}{4 N_\sigma^3 N_\tau} \langle \mathrm{Tr} D_l^{-2} \rangle \tag{12}$$

Here D_l denotes the light quark, staggered fermion Dirac matrix. A crucial role in the analysis of the temperature dependence of the axial anomaly and its overall strength is played by the disconnected chiral susceptibility in the following way.

$U(1)_A$ symmetry relates the susceptibilities of the pion and the scalar iso-triplet delta meson. In a chirally symmetric system one has the degeneracy between pion and iso-scalar meson whose susceptibility is the same as the chiral susceptibility. The disconnected chiral susceptibility, $\chi_{l,disc}$, is directly related to $U(1)_A$ in the following way,

$$\begin{aligned} \chi_\pi - \chi_\delta &= \chi_{l,disc} + (\chi_\pi - \chi_\sigma) \\ &= \chi_{l,disc}, \quad \text{in chirally restored phase} \end{aligned} \tag{13}$$

which says in a chirally symmetric background $\chi_{l,disc}$ vanishes when $U(1)_A$ is effectively restored. This is the strategy we are going to take and here we present some preliminary results in this direction.

3.2 Results

Existing calculations with staggered fermions[19–21] as well as overlap and Möbius domain wall[22–24] and Wilson[25] fermions show evidence for effective restoration of anomalous $U_A(1)$ symmetry above the pseudo-critical temperature T_{pc}, *i. e.* at about $(1.2 - 1.3)T_{pc}$.

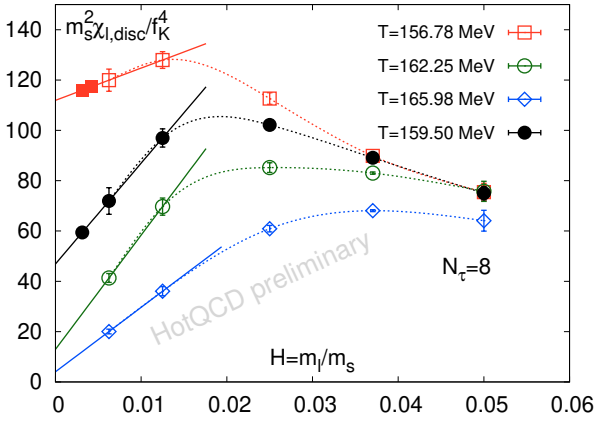

Figure 10. The quark mass dependence of the disconnected chiral susceptibility at three values of the temperature obtained on lattices of size $N_\sigma^3 \times 8$ with $N_\sigma = 32 - 56$. Shown are results for a light (m_l) to strange (m_s) quark mass ratio $1/160 \leq m_l/m_s \leq 1/20$. The open symbols are the data points on which direct calculation is available and solid symbols correspond to those points where interpolation or extrapolation has been used. Dotted lines are drawn to guide the eye and the solid lines are drawn from a linear fit using the points corresponding to $H = 1/80$ and $H = 1/160$.

At non-zero values of the light quark masses the disconnected chiral susceptibility $\chi_{l,disc}(T)$ and the total chiral susceptibility $\chi_m(T)$ share the same qualitative properties, *i. e.* $\chi_{dis}(T)$ has a pronounced peak close to that of the total chiral susceptibility which also rises with decreasing values of the quark mass. When one approaches the chiral limit these two peaks start coming more close to each other and in the chiral limit both total and disconnected chiral susceptibility diverges at T_c^0. In particular, the location of the peak in $\chi_{l,disc}$ has also been used in calculations with chiral fermions (Domain Wall Fermions) to locate the QCD transition temperature.[26] Also in the chiral limit, it generally is expected that $\chi_{l,disc}$ remains non-zero in the high temperature chirally symmetric phase and that it diverges as the chiral phase transition temperature is approached from above. In Fig. 9 we show the quark mass dependence of the disconnected chiral susceptibility obtained from calculations in (2+1)-flavour QCD with the HISQ action on lattices of $N_\tau = 8$, where the above-mentioned properties are apparent. While the figure shows in the vicinity of the transition temperature the expected quark mass dependence, *i. e.* $\chi_{l,disc}$ rises with decreasing quark mass, the figure also shows that at temperatures $T \gtrsim 165$ MeV the quark mass dependence in the chiral susceptibility seems to be inverted. The disconnected chiral susceptibility becomes smaller as the quark mass decreases.

In Fig. 10 we show preliminary results of $\chi_{l,disc}$ as a function of scaled light quark masses for various temperatures which are above chiral critical temperature, obtained on lattices with temporal extent $N_\tau = 8$ and spatial lattice sizes up to $N_\sigma = 56$. Some of these high temperature results, in particular checks on their insensitivity to finite volume effects have been confirmed.[13] One can see at $T \geq 162$ MeV that $\chi_{l,disc}$ almost monotonically decreases and the trend suggests that in the chiral limit within uncertainty it will vanish. Although the situation becomes more involved for $T \leq 160$ MeV when $\chi_{l,disc}$

first increases with decreasing quark mass and attains a maximum and then sharply decreases. Preliminary calculations of Fig. 10 suggest that for a range of temperatures below 160 MeV that $\chi_{l,disc}$ will still go to zero after proper chiral extrapolation but for even lower temperatures chiral extrapolation will give a finite intercept. In other words, from Fig. 10, it seems to be quite unlikely that $\chi_{l,disc}$ will vanish in chiral limit down to $T = T_c^0$. More calculations are needed to confirm this.

4 Conclusions

Based on two novel estimators, we have calculated the chiral phase transition temperature in QCD with two massless light quarks and a physical strange quark. Eq. 9 lists our thermodynamic-, continuum- and chiral- extrapolated result for the chiral phase transition temperature, which is about 25 MeV smaller than the pseudo-critical (crossover) temperature, T_{pc} for physical values of the light and strange quark masses. Preliminary calculations of disconnected chiral susceptibility suggests that in $U_A(1)$ the symmetry remains broken at chiral phase transition.

Acknowledgements

This work was supported in part by the Deutsche Forschungsgemeinschaft (DFG) through the grant 315477589-TRR 211, the grant 05P18PBCA1 of the German Bundesministerium für Bildung und Forschung, grant 283286 of the European Union, the National Natural Science Foundation of China under grant numbers 11775096 and 11535012, Furthermore, this work was supported through Contract No. DE-SC0012704 with the U.S. Department of Energy, through the Scientific Discovery through Advanced Computing (SciDAC) program funded by the U.S. Department of Energy, Office of Science, Advanced Scientific Computing Research and Nuclear Physics and the DOE Office of Nuclear Physics funded BEST topical collaboration, and a Early Career Research Award of the Science and Engineering Research Board of the Government of India. Numerical calculations have been made possible through PRACE grants at CSCS, Switzerland, and at the Gauss Centre for Supercomputing and NIC-Jülich, Germany as well as grants at CINECA, Italy. These grants provided access to resources on Piz Daint at CSCS, at JUWELS at NIC as well as on Marconi at CINECA. Additional calculations have been performed on GPU clusters of USQCD, at Bielefeld University, the PC^2 Paderborn University and the Nuclear Science Computing Center at Central China Normal University, Wuhan, China. Some data sets have also partly been produced at the TianHe II Supercomputing Center in Guangzhou.

References

1. For a recent review see: H. T. Ding, F. Karsch, and S. Mukherjee, *Thermodynamics of strong-interaction matter from Lattice QCD*, Int. J. Mod. Phys. E **24**, 1530007, 2015, arXiv:1504.05274 [hep-lat].
2. Y. Aoki, S. Borsanyi, S. Durr, Z. Fodor, S. D. Katz, S. Krieg, and K. K. Szabo, *The QCD transition temperature: results with physical masses in the continuum limit II.*, JHEP **0906**, 088, 2009, arXiv:0903.4155 [hep-lat].

3. A. Bazavov *et al.*, *The chiral and deconfinement aspects of the QCD transition*, Phys. Rev. D **85**, 054503, 2012, arXiv:1111.1710 [hep-lat].
4. C. Bonati, M. D'Elia, M. Mariti, M. Mesiti, F. Negro, and F. Sanfilippo, *Curvature of the chiral pseudocritical line in QCD: Continuum extrapolated results*, Phys. Rev. D **92**, 054503, 2015, arXiv:1507.03571 [hep-lat].
5. A. Bazavov *et al.* [HotQCD Collaboration], *Chiral crossover in QCD at zero and non-zero chemical potentials*, Phys. Lett. B **795** 15, 2019, arXiv:1812.08235 [hep-lat].
6. R. D. Pisarski and F. Wilczek, *Remarks on the Chiral Phase Transition in Chromodynamics*, Phys. Rev. D **29**, 338, 1984.
7. A. Butti, A. Pelissetto, and E. Vicari, JHEP **0308**, 029, 2003.
8. M. Grahl and D. H. Rischke, *Functional renormalization group study of the two-flavor linear sigma model in the presence of the axial anomaly*, Phys. Rev. D **88**, 056014, 2013, arXiv:1307.2184 [hep-th].
9. A. Pelissetto and E. Vicari, *Relevance of the axial anomaly at the finite-temperature chiral transition in QCD*, Phys. Rev. D **88**, 105018, 2013, arXiv:1309.5446 [hep-lat].
10. T. Sato and N. Yamada, *Linking $U(2) \times U(2)$ to $O(4)$ model via decoupling*, Phys. Rev. D **91**, 034025, 2015, doi:10.1103/PhysRevD.91.034025, arXiv:1412.8026 [hep-lat].
11. M. Hasenbusch, *Eliminating leading corrections to scaling in the three-dimensional O(N) symmetric ϕ^4 model: N=3 and 4*, J. Phys. A **34**, 8221, 2001, arXiv:cond-mat/0010463].
12. J. Engels, S. Holtmann, T. Mendes, and T. Schulze, *Equation of state and Goldstone mode effects of the three-dimensional O(2) model*, Phys. Lett. B **492**, 219, 2000, arXiv:hep-lat/0006023.
13. H. T. Ding *et al.* [HotQCD Collaboration], *Chiral Phase Transition Temperature in (2+1)-Flavor QCD*, Phys. Rev. Lett. **123**, 062002, 2019, arXiv:1903.04801 [hep-lat].
14. H.-T. Ding, P. Hegde, F. Karsch, A. Lahiri, S.-T. Li, S. Mukherjee, and P. Petreczky, *Chiral phase transition of (2+1)-flavor QCD*, Nucl. Phys. A **982**, 211, 2019, arXiv:1807.05727 [hep-lat].
15. F. Karsch and E. Laermann, *Susceptibilities, the specific heat and a cumulant in two flavor QCD*, Phys. Rev. D **50**, 6954, 1994, arXiv:hep-lat/9406008.
16. J. Engels and F. Karsch, *Finite size dependence of scaling functions of the three-dimensional O(4) model in an external field*, Phys. Rev. D **90**, 014501, 2014, arXiv:1402.5302 [hep-lat].
17. E. Follana *et al.* [HPQCD and UKQCD Collaborations], *Highly improved staggered quarks on the lattice, with applications to charm physics*, Phys. Rev. D **75**, 054502, 2007, arXiv:hep-lat/0610092.
18. For details on the tuning of quark masses, determination of lines of constant physics and scale setting using the kaon decay constant used in our calculations see: A. Bazavov *et al.* [HotQCD Collaboration], *Equation of state in (2+1)-flavor QCD*, Phys. Rev. D **90**, 094503, 2014, arXiv:1407.6387 [hep-lat].
19. A. Bazavov *et al.*, *Meson Screening Masses in (2+1)-Flavor QCD*, arXiv:1908.09552 [hep-lat].
20. M. Cheng *et al.*, *Meson screening masses from lattice QCD with two light and the strange quark*, Eur. Phys. J. C **71**, 1564, 2011, doi:10.1140/epjc/s10052-011-1564-y, arXiv:1010.1216 [hep-lat].

21. H. Ohno, U. M. Heller, F. Karsch, and S. Mukherjee, $U_A(1)$ *breaking at finite temperature from the Dirac spectrum with the dynamical HISQ action*, PoS LAT **2012** , 095, 2012, doi:10.22323/1.164.0095, arXiv:1211.2591 [hep-lat].
22. M. I. Buchoff *et al.*, *QCD chiral transition,* $U(1)_A$ *symmetry and the dirac spectrum using domain wall fermions*, Phys. Rev. D **89**, 054514, 2014, doi:10.1103/PhysRevD.89.054514, arXiv:1309.4149 [hep-lat].
23. A. Bazavov *et al.* [HotQCD Collaboration], *The chiral transition and* $U(1)_A$ *symmetry restoration from lattice QCD using Domain Wall Fermions*, Phys. Rev. D **86**, 094503, 2012, doi:10.1103/PhysRevD.86.094503, arXiv:1205.3535 [hep-lat].
24. A. Tomiya, G. Cossu, S. Aoki, H. Fukaya, S. Hashimoto, T. Kaneko, and J. Noaki, *Evidence of effective axial U(1) symmetry restoration at high temperature QCD*, Phys. Rev. D **96**, 034509, 2017, doi:10.1103/PhysRevD.96.034509, [Addendum: Phys. Rev. D **96**, 079902, 2017, doi:10.1103/PhysRevD.96.079902], arXiv:1612.01908 [hep-lat].
25. B. B. Brandt, A. Francis, H. B. Meyer, O. Philipsen, D. Robaina, and H. Wittig, *On the strength of the* $U_A(1)$ *anomaly at the chiral phase transition in* $N_f = 2$ *QCD*, JHEP **1612**, 158, 2016, doi:10.1007/JHEP12(2016)158, arXiv:1608.06882 [hep-lat].
26. T. Bhattacharya *et al.*, *QCD Phase Transition with Chiral Quarks and Physical Quark Masses*, Phys. Rev. Lett. **113**, 082001, 2014, doi:10.1103/PhysRevLett.113.082001, arXiv:1402.5175 [hep-lat].